Determinants of cytoplasmic microtubule reorganization during ciliogenesis in *Chlamydomonas reinhardtii*

Larissa L Dougherty[1], Prachee Avasthi[1,,§,*]

[1]Biochemistry and Cell Biology Department, Geisel School of Medicine at Dartmouth College, Hanover, New Hampshire
[§]Address correspondence to prachee.avasthi@dartmouth.edu at Geisel School of Medicine at Dartmouth College
[*]Prachee Avasthi is the CSO at Arcadia Science

Abbreviations

- CMTs = Cytoplasmic Microtubules
- IFT = Intraflagellar Transport
- MS = Mechanical Shear
- PTX = Paclitaxel

ABSTRACT

At the core of cilia are microtubules which are important for establishing length and assisting ciliary assembly and disassembly; however, another role for microtubule regulation on ciliogenesis lies outside of the cilium. The microtubule cytoskeleton is a highly dynamic structure which reorganizes rapidly to assist in cellular processes. Cytoplasmic microtubule dynamics have previously been thought to be necessary to free up tubulin and proteins in the ciliary precursor pool for ciliogenesis. However, we previously found that low concentrations of taxol can stabilize cytoplasmic microtubules during deciliation while allowing normal cilium regrowth. Here we look at the relationship between ciliogenesis and cytoplasmic microtubule dynamics in *Chlamydomonas reinhardtii* using chemical and mechanical perturbations. We find that not only can stabilized cytoplasmic microtubules allow for normal ciliary assembly, but high calcium concentrations and low pH-induced deciliation cause microtubules to depolymerize separately from ciliary shedding. In addition, we find that through mechanical shearing, cilia regenerate more quickly despite intact cytoplasmic microtubules. Our data suggests that cytoplasmic microtubules are not a sink for a limiting pool of cytoplasmic tubulin, reorganization that occurs following deciliation is a consequence rather than a requirement for ciliogenesis, and intact microtubules in the cytoplasm and the proximal cilium support more efficient ciliary assembly.

INTRODUCTION

Ciliogenesis describes the formation of cilia which are microtubule extensions from the plasma membrane that serve as signaling and sometimes motile components of quiescent cells (Tucker et al., 1979). These largely microtubule-based structures are assembled and maintained through intraflagellar transport (IFT) where tubulin monomers among other components are taken to the tip of the cilium and back to the base by protein complexes (Craft et al., 2015; Kozminski et al., 1993). This process is influenced by not only the core proteins required for IFT, but also ciliary gene transcription, protein synthesis, trafficking, and complex pre-assembly occurring outside of the cilium. All of the required structures and components generate a highly regulated structure and signaling environment within cilia, and because of this, disruptions to any of these components can lead to various diseases (Reiter & Leroux, 2017). Therefore, it is important to understand how manipulation of cellular processes and components can influence ciliary assembly.

While cilia are themselves a microtubule superstructure, microtubules are also highly dynamic components elsewhere in the cell. They provide structure and polarity to the cell, serve as highways for molecular trafficking, and facilitate cell division among many other roles(de Forges et al., 2012; Parker et al., 2014). To serve these many roles, tubulin assembles and disassembles very rapidly through the process of dynamic instability which describes how tubulin can disassemble into monomers very quickly from GTP hydrolysis (Alushin et al., 2014; Mitchison & Kirschner, 1984).

Disruption of microtubule dynamics has been shown to directly impact the ability for cilia to assemble. For example, through the use of microtubule inhibitors such as colchicine or colcemid, cilia cannot assemble at all in Chinese hamster fibroblasts (Stubblefield & Brinkley, 1966) *Chlamydomonas* (Rosenbaum et al., 1969) and *Tetrahymena* (Rosenbaum & Carlson, 1969). Conversely, use of the microtubule stabilizer, taxol, has more recently been shown to inhibit acute ciliary elongation in *Chlamydomonas reinhardtii* (Wang et al., 2013). However, while microtubule destabilizing drugs were found to inhibit ciliary assembly, taxol was previously not found to have any effects in PtK1 cells on either assembly or disassembly of primary cilia (Jensen et al., 1987). In contrast, taxol can prevent actin stabilization and depolymerization-induced ciliary elongation through forskolin, jasplakinolide, and the PKA inhibitor CD. Consistently, the MT depolymerizing drug nocodazole was shown to increase ciliary length likely by freeing up tubulin for ciliogenesis in RPE cells whereas taxol itself also shortens cilia (Sharma et al., 2011). Given these cell-type specific and chemical specific discrepancies describing the interplay between cytoplasmic microtubule dynamics and ciliary dynamics, it is important to continue investigating how these processes impact one another to better understand how ciliary dynamics are regulated.

Microtubule dynamics with respect to ciliary dynamics have predominantly been studied through chemical perturbations. Here we explore the requirement for microtubule dynamics in the ciliary model organism *Chlamydomonas reinhardtii* with both chemical perturbations in addition to mechanical perturbations to better understand how microtubule dynamics can regulate ciliary assembly.

RESULTS AND DISCUSSION

It has previously been shown that 40 μM paclitaxel (PTX), a microtubule stabilizer, inhibits ciliary elongation through lithium chloride and stunts ciliary length when grown from zero length (Wang et al., 2013). However, we found in our previous work that a lower paclitaxel concentration, 15 μM PTX, can allow for normal ciliary elongation following pH shock in *Chlamydomonas* (Dougherty et al., 2023). In addition, it is well known that higher concentrations of taxol, a paclitaxel equivalent, can induce different processes from lower concentrations, and lower concentrations of taxol can inhibit microtubule dynamics without altering tubulin polymer mass which occurs with higher concentrations (Derry et al., 1998; Jordan et al., 1993). Taxol can also differentially impact microtubule processivity depending on the organism and tubulin isoform (Chew & Cross, 2023).

To test if taxol is indeed stabilizing microtubules at lower concentrations in *Chlamydomonas reinhardtii*, we isolated the soluble ("S") and insoluble ("P") β-tubulin fractions after treating cells with DMSO, 15 μM PTX, 40 μM PTX, 2 mg/mL colchicine, or 0.5M acetic acid to induce deciliation ("pH shock") (**Figure 1A**). Following PTX treatment, both 15 μM and 40 μM PTX increased the presence of β-tubulin in the soluble fraction, confirming that both concentrations sufficiently stabilize microtubules in the cells (**Figure 1A and 1B**). To directly compare the effect of PTX on acute ciliogenesis extending beyond steady-state length, cells were treated with increasing concentrations of PTX in the presence or absence of 25 mM lithium chloride (LiCl) (Nakamura et al., 1987). Regardless of PTX concentration, cilia significantly elongated in the presence of LiCl in the CC-1690 wild-type strain in M1 liquid media (**Figure 1C**) previously used in (Wang et al., 2013). We also checked the ability for cilia to completely regenerate from zero length through pH shock which involves dropping the cell suspension pH to 4.5 for 45 seconds with 0.5 M acetic acid and returning the pH to 7.0 with 0.5 M KOH (Witman et al., 1972) in the presence of 15 μM PTX (confirmed to stabilize microtubules at this concentration), 40 μM PTX, or 60 μM PTX compared to control cells in DMSO (Figure 1D). Similarly and consistent with our previous work (Dougherty et al., 2023), cilia regenerated normally in 15 μM PTX, though even at 60 μM PTX, ciliary length did not differ from DMSO treated cells at 120m (**Figure 1D**). To compare the ability for PTX to stabilize microtubules during pH shock, we pretreated cells for 10 min with PTX and before pH shock and then fixed and stained them for beta tubulin within 5 minutes when microtubules are normally depolymerized (**Figure 1E**). We found that, even immediately following deciliation, microtubules are stabilized similarly to pre-deciliated cells (**Figure 1F**). Our data do not recapitulate the ciliary regrowth inhibition seen in Wang et al., 2013, and suggest that PTX stabilized cytoplasmic microtubules do not prevent acute ciliary assembly.

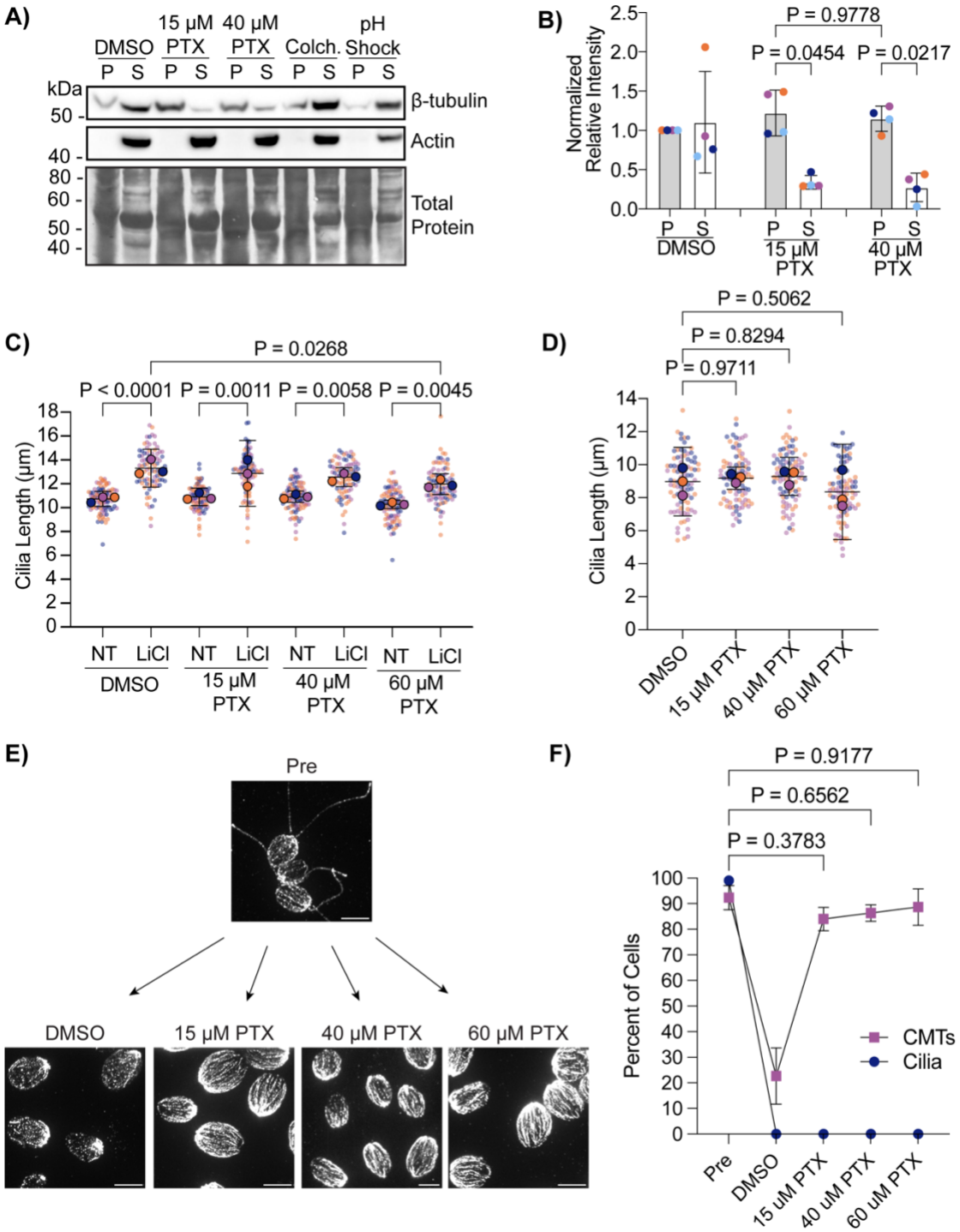

Figure 1. Lower concentrations of taxol stabilize cytoplasmic microtubules do not affect ciliogenesis. **A)** Wild-type cells (CC-5325) were treated with 1% DMSO (control), 15 μM paclitaxel (PTX), 40 μM PTX, 2 mg/mL colchicine, or acetic acid to drop the pH of the cells to 4.5 to induce ciliary shedding. Protein was collected and probed for β-tubulin, actin (soluble protein control), or total protein with coomassie on PVDF membrane. **B)** Quantification of DMSO or PTX bands in (A). Significance was determined with a One-Way ANOVA (N=3). Error bars are mean with standard deviation. For all tests, P<0.05 is considered significantly different. **C)** Wild-type cells (CC-1690) were grown in M1 media overnight and then treated with 1% DMSO or increasing concentrations of PTX with

188 or without 25 mM LiCl for 30 min. Significance was determined with a One-Way ANOVA and Šídák's
189 multiple comparisons test (n=30, N=3). **D)** Wild-type cells (CC-5325) were grown in TAP media overnight,
190 pretreated in increasing concentrations of PTX for 10 min, and then regenerated for 2 h after pH shock
191 with acetic acid. Significance was determined with a One-Way ANOVA and Šídák's multiple comparisons
192 test (n=30, N=2). Error bars are mean with 95% confidence interval. **E)** Representative images of beta
193 tubulin stained cells at the 5 min timepoint post pH shock in (D). Scale bars are 5 µm. **F)** Quantification of
194 the percent of cells with cilia and polymerized cytoplasmic microtubules (CMTs) at 120 min post pH shock
195 in taxol. Navy blue circles are cilia; purple squares are CMTs. Error bars are mean with standard
196 deviation (n=100, N=3).Significance for CMTs is represented on the graph and determined using a One
197 Way ANOVA with Šídák's multiple comparisons test.
198
199 While deciliation and regrowth of cilia from zero length is coincident with
200 cytoplasmic microtubule depolymerization and stabilization of these microtubules does
201 not affect cilium regrowth, we wondered whether acute cilium growth from steady state
202 showed similar patterns of microtubule reorganization. Acute growth from multiple
203 lengths may indicate whether cytoplasmic microtubule depolymerization is specific to
204 cilium growth or decollation.. Using 25 mM LiCl to induce ciliary elongation, we checked
205 the status of cytoplasmic microtubules across 30 minutes during treatment (**Figure 2A**).
206 Throughout this time, cells were able to elongate ~2 µm as reported in Wang et al.,
207 2013 (**Figure 2B**). However, upon checking cytoplasmic microtubule status throughout
208 this process, we find that these microtubule arrays remained undisturbed in both
209 untreated and LiCl treated cells (**Figure 2C**). This data suggests that microtubule
210 reorganization is not necessary for ciliary assembly, though it is possible that finer
211 microtubule reorganization could occur on a level that is not detectable with these
212 methods.

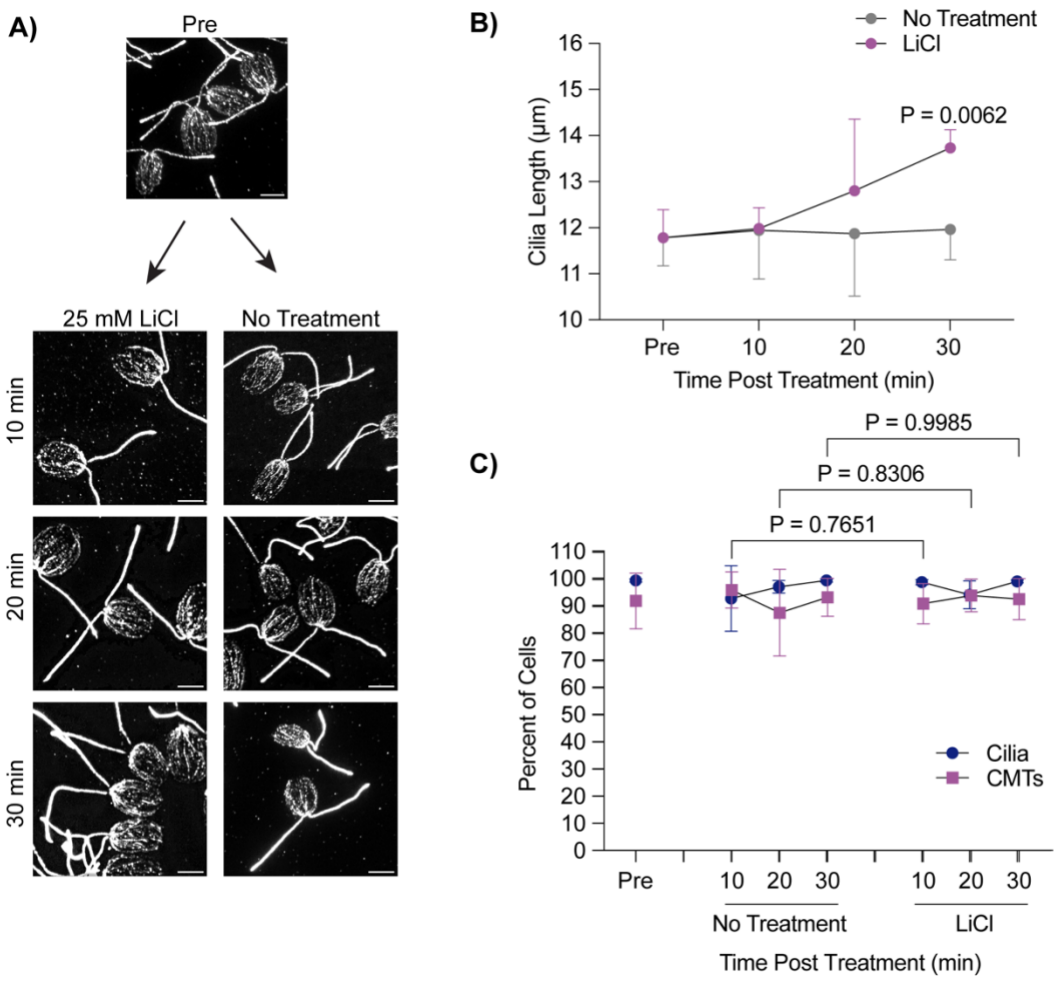

Figure 2. Lithium Chloride-induced ciliary elongation does not require microtubule depolymerization. A) Wild-type cells were treated with either 25 mM LiCl or nothing for 30 minutes and then fixed and stained for beta Tubulin. Scale bars are 5 µm. **B)** Quantification of cilia length for the experiment described in (A). Error bars are mean with 95% confidence interval (n=30, N=3). Significance compares cilia length at 30 min between treatments and was determined with a Two Way ANOVA with Šídák's multiple comparisons test. **C**) Quantification of percent of cells with cilia versus polymerized microtubules for the experiment described in (A). Error bars are mean with standard deviation (n=100, N=3). Significance for CMTs is represented on the graph and determined using a One-Way ANOVA with Šídák's multiple comparisons test.

Ciliary shedding is also commonly induced through pH shocking cells (Witman et al., 1972). Microtubules depolymerize during pH shock-induced ciliary shedding (Wang et al., 2013) (**Figure 1A and Figure 1F**) but do not depolymerize during LiCl induced ciliary elongation (**Figure 2**). Our data suggests that ciliary loss may trigger depolymerization rather than polymerization. To better understand if depolymerization is a result of physical loss of the cilium versus other factors coincident with cilium loss, we utilized a previously characterized *fa2* mutant which has a mutation in the microtubule severing protein at the base of the cilium, katanin, which prevents ciliary shedding in the presence of acid (Finst et al., 1998) (**Figure 3A**). Following pH shock, we found that while wild-type cells shed 100% of their cilia and depolymerized ~70% of their

cytoplasmic microtubules (**Figure 3B, left**), the katanin mutants maintained ciliated cells as expected, but surprisingly also depolymerized microtubules similar to wild-type (**Figure 3B, right**). Also interestingly, wild-type cells were able to reform their cytoplasmic microtubules within 10 minutes whereas ciliogenesis does not begin until between 20 and 30 minutes. This data shows that the presence of microtubules does not inhibit assembly given that microtubules are present at the time that ciliogenesis initiates.

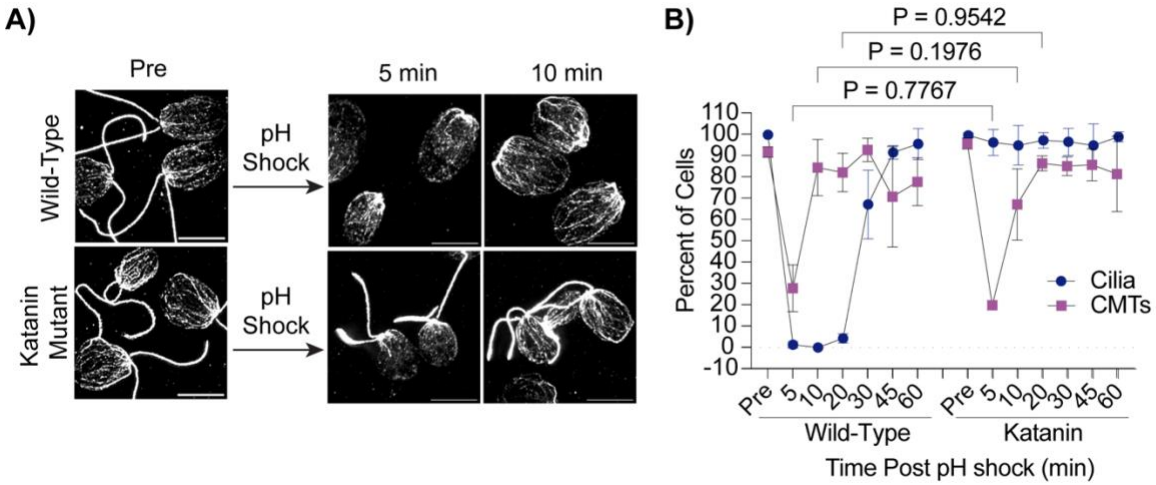

Figure 3. Cilium loss is not required for microtubule depolymerization with pH shock. A) Wild-type or Katanin mutants (*fa2*) were pH shocked with acetic acid for 45 sec and then regrown in fresh tap for 60 min. Cells were fixed and stained for beta tubulin. Scale bars are 5 µm. **B)** Quantification of percent of cells with cilia or CMTs post pH shock. Error bars are mean with standard deviation (n=100, N=3). Significance was determined with a One-Way ANOVA and Šídák's multiple comparisons test.

It has previously been established that pH shock induces a calcium influx into the cell (L. M. Quarmby, 1996), and introducing the cell to higher concentrations of calcium can induce ciliary shedding (L. Quarmby & Hartzell, 1994). To further test what triggers microtubule reorganization coincident with deciliation we tested if calcium influx, known to occur upon pH shock was sufficient to induce cytoplasmic microtubule depolymerization. We introduced cells to 75 mM calcium chloride in 5 mM HEPES ("Buffer") for 10 minutes which is long enough to induce robust ciliary shedding. Following ciliary shedding, cilia regenerated similar to cilia exposed to pH shock (**Figure 4A**). We then measured the effect of calcium induced ciliary shedding on cytoplasmic microtubule stability. Upon ciliary shedding, we found that cytoplasmic microtubules also depolymerized quickly and then reformed similar to pH shock (**Figure 4B).** To determine if calcium has the same effect on ciliated cells, we repeated this experiment in katanin mutants (**Figure 4C-E**). Similar to wild-type cells, katanin mutants also exhibited depolymerized microtubules though they did not depolymerize to the same degree as wild-type (**Figure 4E**). It is possible that microtubule depolymerization could be occurring through similar mechanisms. It has previously been found that pH shock

268 induces a calcium influx to activate katanins for ciliary severing (L. Quarmby & Hartzell,
269 1994). By flooding the extracellular matrix with high concentrations of calcium, it is
270 possible that this is sufficient for calcium influx into the cell to activate the same
271 pathways. In addition, it has previously been found that calcium destabilizes microtubule
272 plus end growth (O'Brien et al., 1997). Calcium influx into the cell may be inducing
273 multiple independent events within the cell.
274

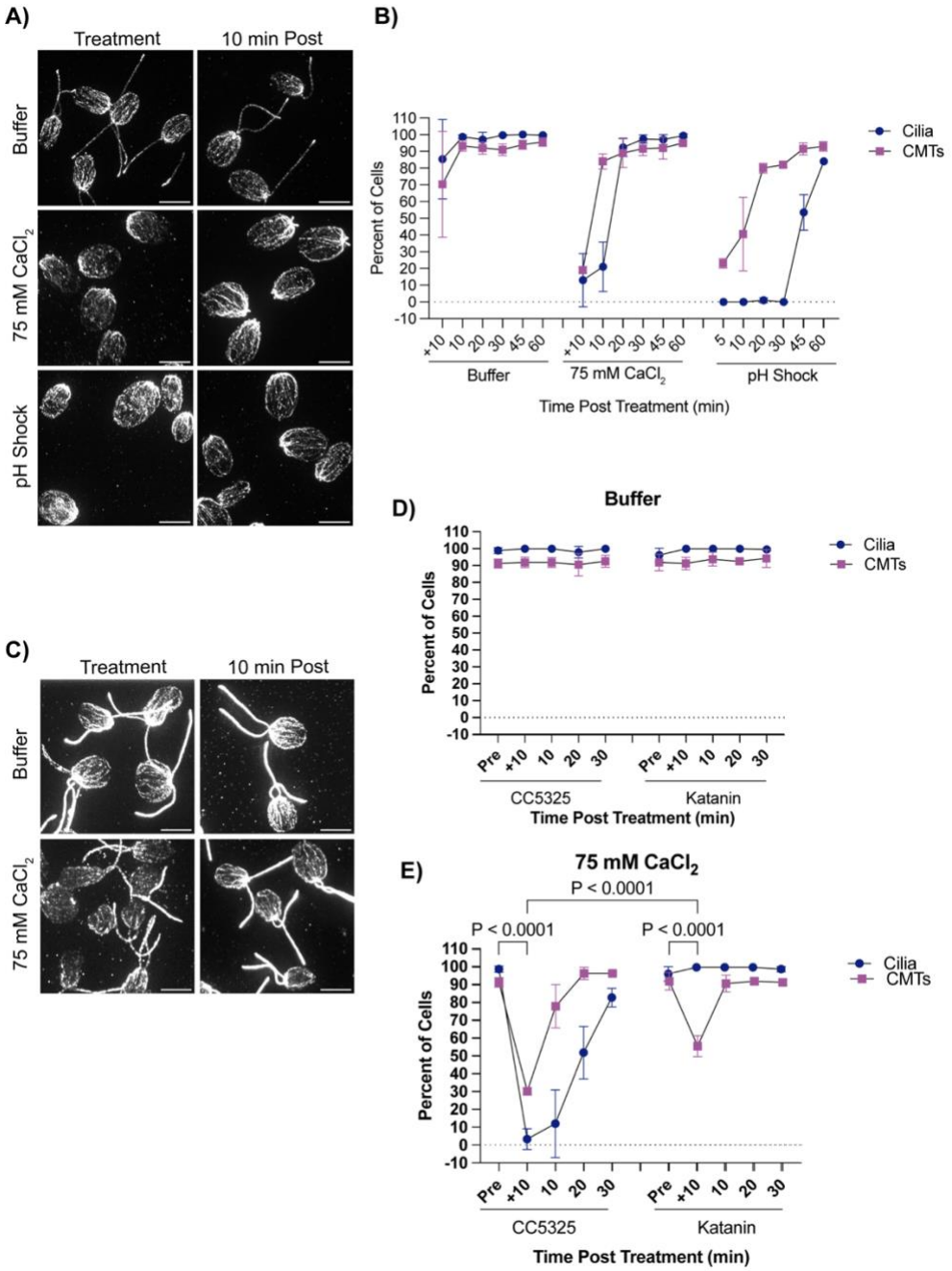

275
276 **Figure 4. Cilium loss is not required for microtubule depolymerization with**
277 **calcium induction. A)** Wild-type cells were either pretreated for 10 minutes in 5 mM HEPES
278 ("Buffer"), 10 minutes in 75 mM CaCl2, or 45 seconds in acetic acid, and then fixed and stained for beta
279 tubulin. Scale bars are 5 µm. **B)** Quantification of cilia and CMTs from (A). Error bars are mean with

standard deviation (n=100, N=3). **C)** Representative images of Katanin mutants following treatment in buffer or 75 mM calcium chloride. Cells were fixed and stained for beta tubulin. Scale bars are 5 µm. **D-E**) Quantification of CC-5325 or Katanin mutants in buffer (**C**) or 75 mM CaCl2 **(E)**. Error bars are mean with standard deviation (n=100, N=3) for the experiment described in (**C**). Statistics compare CMTs and were determined using a One-Way ANOVA and Šídák's multiple comparisons test.

Introducing different chemicals to cells to induce ciliary shedding induces differential effects on stability of cytoplasmic microtubules. We wanted to assess cytoplasmic microtubule stability without the use of chemicals. We introduced the cells to a cell homogenizer/bead beater for 3 minutes to excise cilia and then looked at cytoplasmic microtubules as cilia regenerated (**Figure 5A**). Interestingly, mechanical shearing did not induce robust cytoplasmic microtubule depolymerization (**Figure 5B**). Further, mechanically sheared cilia were able to regenerate back to full length much faster (in 60 minutes) whereas cilia shed via pH shock were only able to regenerate to half-length in this time (**Figure 5C**). Looking more closely at regeneration in these processes, we found that mechanically sheared cilia, which maintain a ~1 µm ciliary track immediately following ciliary excision, can immediately begin steadily regenerating overtime (**Figure 5C)** at a slower rate (**Figure 5D**). In contrast, pH shocked cells have delayed ciliogenesis, but after this process is started, cells can more rapidly regenerate cilia (**Figure 5B-C**). To confirm that this was not a consequence of cytoplasmic microtubule reestablishment, we compared ciliogenesis to cytoplasmic microtubule organization. Though pH shocked cells reestablished microtubules within 10-20 minutes, ciliogenesis did not continue until 30-45 minutes post deciliation unlike mechanically sheared cells which maintained both cytoplasmic microtubule organization and cilia throughout (**Figure 5B-C**)**.** These data show that in the case where cilium growth happens faster, depolymerization does not occur. Our data may suggest that polymerized cytoplasmic microtubules facilitate more rapid ciliogenesis. Alternatively, the existence of cilium initial segments may promote more rapid assembly completely independent of cytoplasmic microtubules state that is dependent instead upon calcium influx (**Figure 4**) that may not be triggered upon mechanical shearing. It could be that initiation of ciliary assembly is rate limiting.

The delay in ciliary shedding due to pH shock may differentially affect microtubules based on modifications that add stability. To test this, we also compared the presence of acetylated alpha tubulin in pH shocked cells versus mechanically sheared cells. Deacetylation of alpha tubulin has been found to work in concert with ciliary disassembly during mitosis, and acetylation can act as a signal for downstream events such as cell differentiation in adipocytes (Forcioli-Conti et al., 2016). In addition to the ciliary axoneme being heavily comprised of acetylated tubulin, *Chlamydomonas* has 4 rootlet microtubules present at the ciliary base which extend into the cell (Boyd et al., 2011; Dutcher & O'Toole, 2016). Acetylation recruits further modifications to tubulin that allow for motility and ciliary length maintenance in *Chlamydomonas* as well as human cells (Tripathi et al., 2021). It's possible that pH shock could be inducing upstream pathways that inhibit tubulin acetylation must be maintained for ciliogenesis. Comparing pH shock to mechanical shearing, we found that during pH shock, acetylated microtubules were significantly shorter both overall (**Figure 5E and F**) and when comparing the longest rootlet microtubule per cell (**Figure 5E and G**). These data

show that pH shock may affect both stabilized and non-stabilized microtubules or affect the degree of acetylation of the stabilized population.

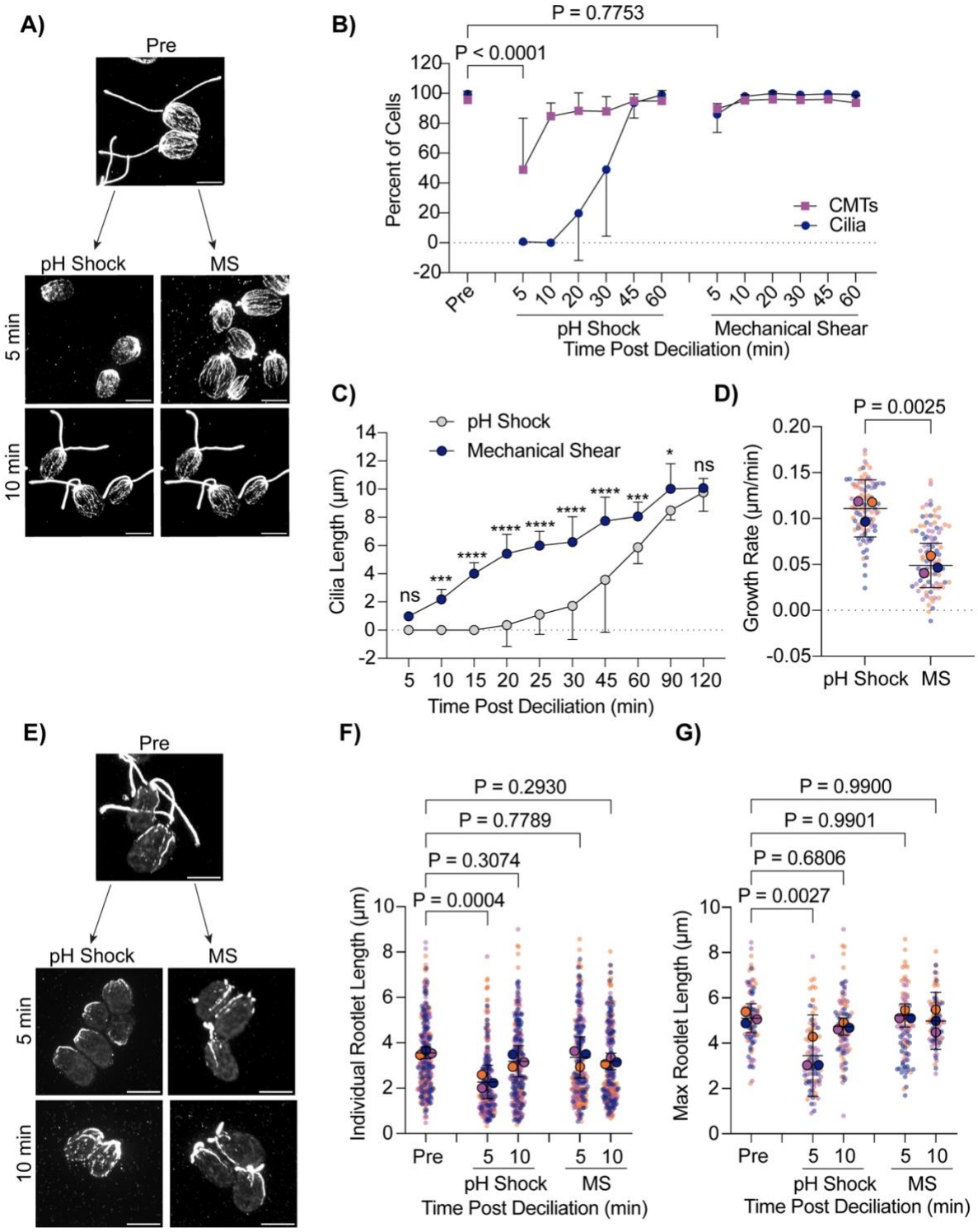

Figure 5. Mechanically sheared cilia do not induce microtubule depolymerization and regenerate more quickly. **A)** Wild-type cells were either pH shocked for 45s or placed in a

cell homogenizer (“Mechanical Shear”, “MS”) for 3 minutes. Representative images are cells fixed and stained for beta tubulin. Scale bars are 5 µm. **B)** Quantification of percent of cells with cilia (navy circles) compared to polymerized microtubules (purple squares) between pH shock (left) and Mechanical Shear (“MS”, right). Error bars are mean with standard deviation. Significance was determined using a One-Way ANOVA and Šídák’s multiple comparisons test (n=30, N=3). **C)** Quantification of cilia length over 2 hours. Error bars are mean with 95% confidence interval (n=30, N=3). Statistics were determined using a Two-Way ANOVA with Šídák’s multiple comparisons test (n=30, N=3). (ns - P>0.05, * P≤0.05, ** P≤0.01, *** P≤0.001, **** P≤0.0001. **D)** Quantification of the ciliary growth rate between pH shock and MS in (**C).** Error bars are mean with 95% interval. P values were measured using a t test (n=30, N=3). **E)** Wild-type cells were fixed and stained for acetylated alpha tubulin following pH shock or MS. Scale bars are 5 µm. **F-G)** Quantification of individual **(F)** or max **(G)** acetylated microtubule rootlet lengths. Error bars are mean with 95% confidence interval. Statistics were determined using a One-Way ANOVA and Dunnett’s multiple comparisons test (n=30 cells, N=3).

Delayed ciliogenesis could indicate that there is a recruitment defect for proteins necessary for ciliogenesis. Using a previously tagged mScarlet-IFT54 anterograde IFT subunit and sfGFP tagged retrograde IFT140 subunit generated and validated by (Wingfield et al., 2021), we compared fluorescence of these complexes at the ciliary base during pH shock and mechanical shear (**Supplemental Figure 1A and 1C**). We found that during pH shock, there is a significant and more robust increase in both anterograde (**Supplemental Figure 1A and 1B**) and retrograde (**Supplemental Figure 1C and 1D**) trafficking complexes during pH shock as compared to mechanical shearing which remains increased during 10 minutes when cytoplasmic microtubules have reformed (**Figure 3B)**. Together, this data suggests that pH shock may cause a delay in ciliogenesis due to altered IFT recruitment at the base of cilia which is required for participation in ciliogenesis. While recruitment is still induced during mechanical shear, there is a ~1 µm track of cilia present for IFT to escape from the basal body area of the cilium which could explain the reduced basal body accumulation due to some IFT components departing for the nascent cilium. This data also may suggest that presence of established microtubules can actually enhance ciliogenesis. It is possible that either through having established acetylated microtubules or cytoplasmic microtubules without acetylation, molecular highways do not have to be rebuilt for proteins from the ciliary precursor pool to be mobilized to the ciliary base.

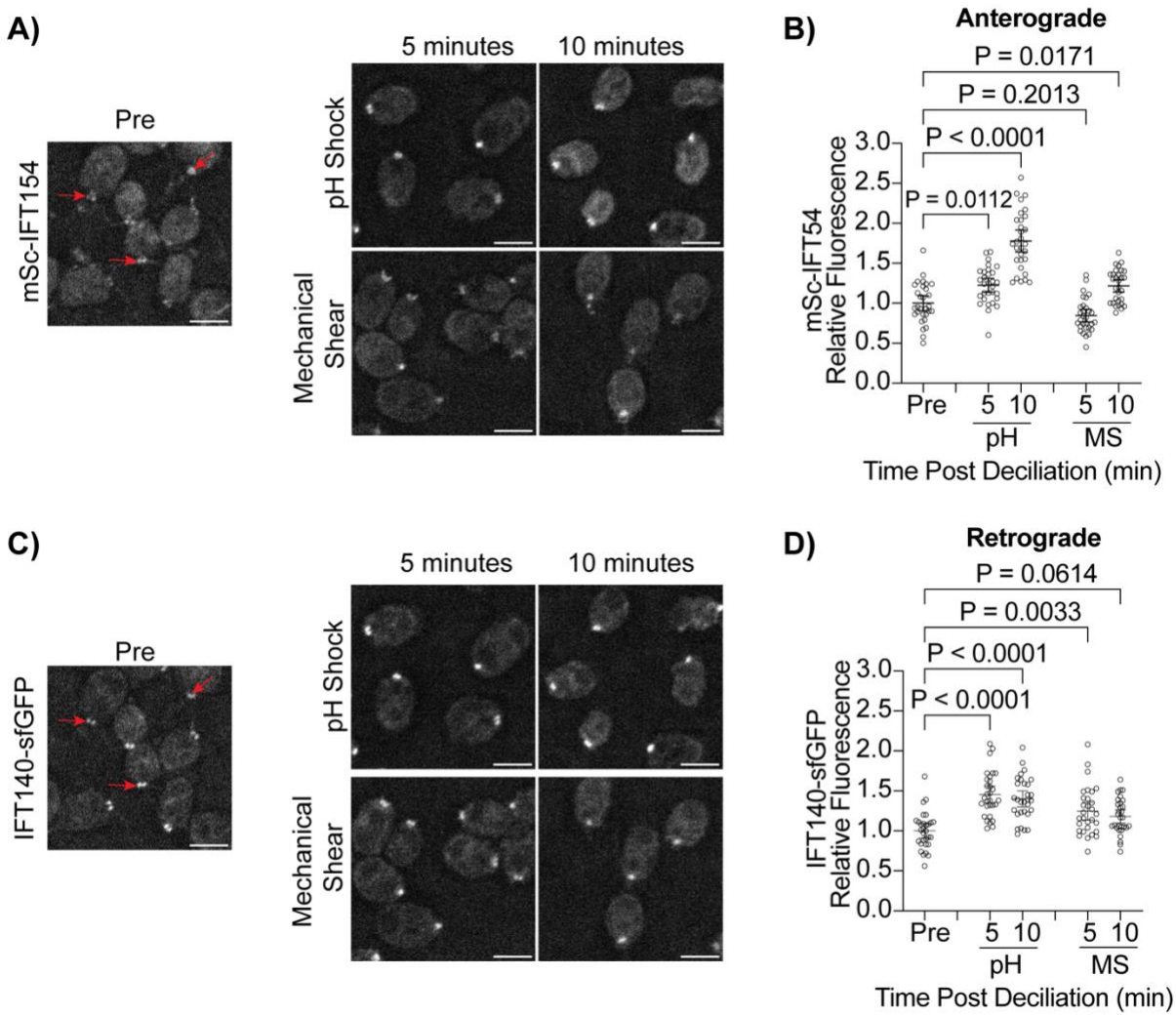

<u>Supplemental Figure 1. PH shock-induced ciliary shedding increases IFT recruitment</u>. **A and C)** mSc-IFT54/IFT140-sfGFP were fixed and imaged. Fluorescence at the base of the cilium was quantified (red arrows). Representative images show cells pre deciliation ("Pre"), 5 minutes, and 10 minutes post treatment for both pH shock and mechanical shear for both mSc-IFT154 (**A**) and IFT140-GFP (**C**) transport. Scale bars are 5 µm. **B and D)** Quantification of mSc-IFT54 (**B**) or IFT140-sfGFP (**D**) fluorescent intensity at the ciliary base. Error bars are mean with 95% confidence interval (n=30, N=1). Statistics were determined using a One-Way ANOVA and Šídák's multiple comparisons test.

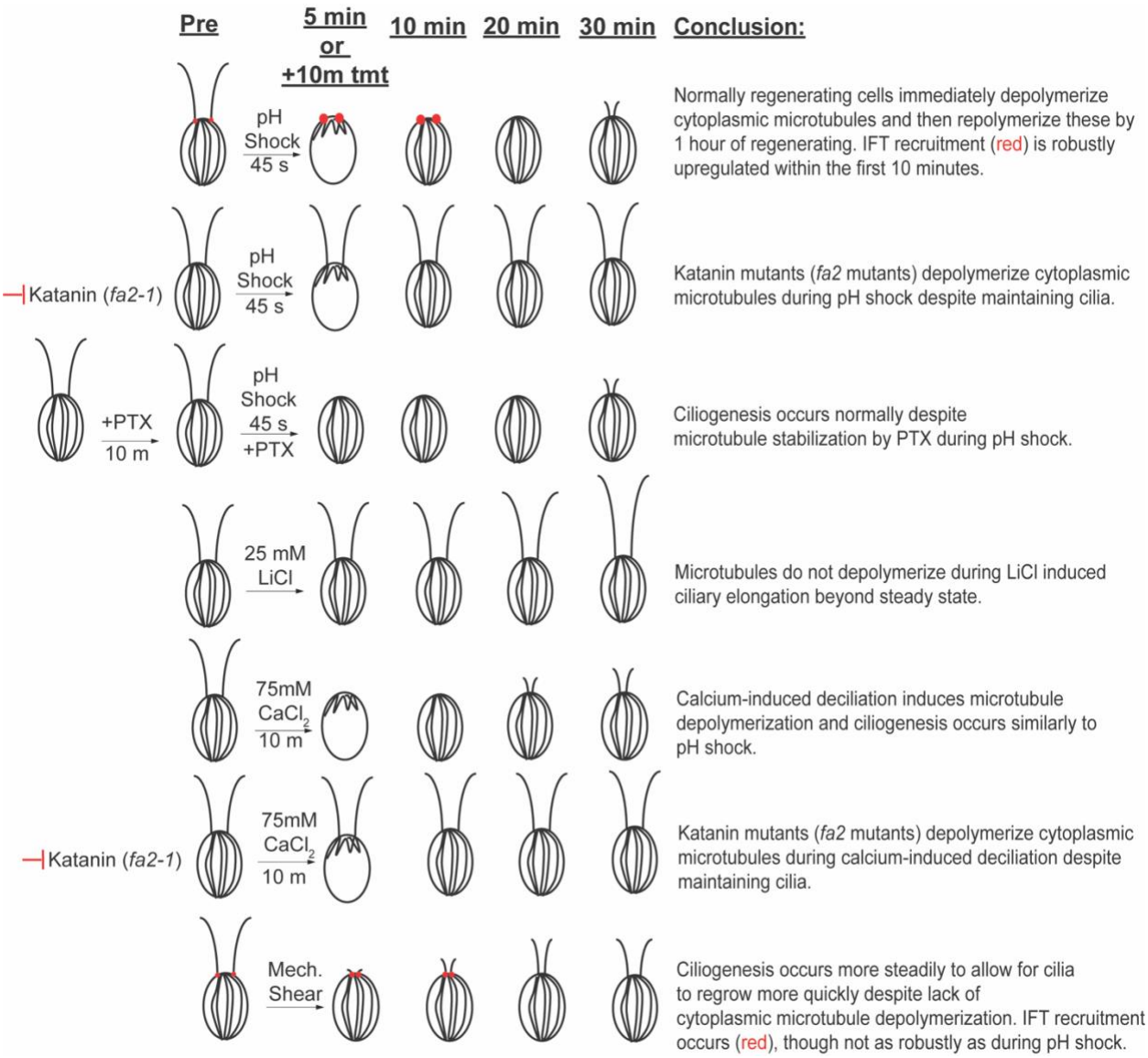

Supplemental Figure 2. Summary of microtubule dynamics in conjunction with ciliogenesis. Results from each trial are summarized for each of the different conditions tested up to 30 minutes. Red dots represent IFT fluorescence tested for both pH shock (top) and mechanical shear (bottom).

Throughout this work, we identify the relationship between ciliogenesis and cytoplasmic microtubule polymerization which we tease apart by holding either of these processes constant while varying possible determinants. We find that while microtubule depolymerization does occur during deciliation with some techniques to induce deciliation, these dynamics are not necessarily required for ciliary assembly and in fact, may inhibit ciliary assembly as we see a reestablishment in acetylated microtubule length before ciliogenesis can begin (**Figure 5 E-G**) and a need for IFT recruitment to the ciliary base (**Supplemental Figure 1**). These findings are summarized in **Supplemental Figure 2**. Our data are consistent with a model in which events happening during deciliation have effects on associated cytoplasmic microtubule processes, but these are not required for ciliogenesis. These data shed light on two

important points: 1) tubulin does not necessarily need to be freed up from the cell in order to allow acute ciliary assembly to occur; and 2) cytoplasmic microtubules are neither required nor block the mobilization of the intracellular pool of ciliary protein precursors which we see through stimulated IFT recruitment both during pH shock and mechanical shearing, though this response is less robust during mechanical shearing.

Effects of pH shock and calcium on live microtubule dynamics alone have been investigated (by Liu et al 2017), however the stability of existing microtubules has not previously been fully explored. Liu et al 2017 found that, by using a Neon-Green tagged EB1 protein, microtubule growth was frozen in *Chlamydomonas* by decreasing pH and increasing calcium concentration. They also noted that the different *Chlamydomonas* tubulin isoforms have different isoelectric points (alpha tubulin = 5.01, beta tubulin = 4.82, and EB1 = 5.7), so dropping the pH below these values which allows for sufficient calcium influx to induce katanins is also sufficient to separately induce microtubule depolymerization, along with the ability for calcium alone to inhibit microtubule dynamics. However, despite the effect of pH on microtubule stability shown in this paper, there is also a considerable lag between the time that microtubules are reestablished the timing of initial ciliogenesis (**Figure 3B and 5B**) which raises the possibility that other signaling pathways that influence ciliogenesis are inhibited during this process. For example, it was previously found that pH shock activates the microtubule depolymerizing kinesin CrKin13 which has also been implicated in ciliogenesis (Wang et al., 2013). Future work needs to be done to better understand how different methods of deciliation can ultimately impact cellular processes that directly regulate ciliogenesis.

MATERIALS AND METHODS

Strains and Maintenance

The wild-type strains (CC-5325 and CC-1690), katanin mutant (fa2-1; CC-3751), and IFT strain (ift140-1::IFT140-sfGFP ift54-2::mS-IFT54 mt; CC-5862) were acquired from the *Chlamydomonas* Resource Center. Cells were maintained on 1.5% Tris Acetate Phosphate (TAP) plates under constant light. For experiments, CC-1690 cells were inoculated into liquid M1 media, and CC-5325 cells, katanin mutant cells, and IFT cells were inoculated in tap and grown overnight under constant light and agitation.

Ciliary Length Experiments

Steady State Ciliary Length Experiments: overnight cultures were resuspended in fresh TAP (or M1 (CC-1690) the next morning. Cells were treated with either DMSO, taxol (PTX), colchicine, or LiCl, fixed in equal amounts of 2% glutaraldehyde, and then imaged on a Zeiss Axioscope 5 DIC with 40x magnification and Zeiss Zen 3.1 software.

PH Shock Induced Ciliary Shedding and Regeneration: overnight cultures were resuspended in fresh TAP and pretreated or not with PTX 10 minutes prior to deciliation. To induce deciliation, 0.5M acetic acid was added to the cell suspension to bring the pH down to 4.5 for 45 sec, and then brought back up to 7.0 with 0.5 M potassium hydroxide. Cells were then spun down at 600xg for 1 minute and resuspended in new tap with or without PTX.

438 **Calcium Chloride-Induced Ciliary Shedding and Regeneration:** overnight
439 cultures resuspended in fresh tap were spun down and resuspended in either 5 mM
440 HEPES or 75 mM calcium chloride in 5 mM HEPES for 10 minutes. Then cells were
441 resuspended in fresh media and allowed to regenerate cilia.
442 **Mechanical Shear-Induced Ciliary Shedding and Regeneration:** Overnight
443 cultures resuspended in fresh tap were placed in a cell homogenizer (Analog Disruptor
444 Genie) for 3 minutes and then resuspended in fresh TAP to regenerate.
445
446 ***Immunofluorescence and Quantification***
447 **Beta Tubulin**: Staining was performed as described in (Wang et al., 2013).
448 Briefly, cells were adhered to poly-lysine coated coverslips, fixed in 30 mM HEPES
449 (pH=7.2), 3 mM EGTA, 1 mM $MgSO_4$, and 25mM KCl with 4% paraformaldehyde
450 ("PFA") for 5 minutes, permeabilized with 0.5% NP-40 for 5 minutes, and then fixed in
451 ice cold methanol for 5 minutes. Coverslips were blocked in 5% BSA and 1% Fish
452 ("Block") gelatin for 30 minutes, then in block with 10% Normal Goat Serum ("NGS",
453 Sigma), and then incubated in beta tubulin (CST, 2146S) diluted in 20% block in PBS
454 overnight at 4˚C. Coverslips were washed 3x10 minutes in PBS, incubated in secondary
455 (Alexafluor 488 goat anti-rabbit IgG, A11008, 1:500) for 1 hour, washed 3x10 minutes in
456 PBS, and allowed to dry. Coverslips were mounted in Fluoromount G (Thermo
457 Scientific) before imaging. Cells were imaged on a Nikon Yokogawa SoRa super
458 resolution spinning disk confocal with 100x oil objective (data collection) and 2.8x
459 magnifier (representative images). For quantification, max IPs were generated from z
460 stacks and 100 cells per time point were counted using the Cell Counter tool in FIJI for
461 either having cytoplasmic microtubules polymerized (spanning > half the cell) or not
462 having microtubules polymerized (spanning < half the cell).
463 **Acetylated Alpha Tubulin**: Cells adhered to coverslips were fixed in 4% PFA in
464 10 mM HEPES for 15 minutes, placed in ice cold 80% acetone for 5 minutes, placed in
465 ice cold 100% acetone for 5 minutes, and then allowed to dry before rehydrating for 5
466 minutes in PBS. Then cells were blocked in 100% Block for 30 minutes, 10% NGS, and
467 stained for acetylated tubulin (1:1000) overnight at 4˚C. Coverslips were washed 3x10
468 minutes in PBS incubated with secondary (Alexa Fluor 499 goat anti-mouse IgG,
469 Invitrogen A11001) for 1h at RT, covered, and then washed 3x10 minutes in PBS,
470 covered before allowing to dry completely and mount with Fluoromount G. For
471 quantification, max IPs were generated and acetylated microtubules were measured
472 using the segmented line tool in FIJI for 30 cells per timepoint.
473 **IFT140/54**: Cells adhered to coverslips were placed in ice cold 100% methanol
474 2x5 minutes, 50% methanol in PBS for 5 minutes, then PBS for 5 minutes before
475 allowing to dry, mount, and image. For quantification, z stacks were summed together,
476 background subtracted with rolling ball radius = 50, and then equal sized circles drawn
477 over the signal at the base of the cilium. Fluorescent intensity was calculated using the
478 calculation for CTCF as previously described (Dougherty et al., 2023)
479
480 ***SDS-PAGE and Immunoblotting***
481 Soluble (S) and insoluble (P) fractions were collected similarly to (Wang et al.,
482 2013). Briefly, treated cells were resuspended in TMMET Buffer with 1 minute of
483 pipetting and 1 minute of gentle vortexing (half-max vortex speed). Cells sat for 10

minutes with 1 gentle round of vortexing before spinning down at 21000xg for 10m, RT. The supernatant was collected ("S" fraction) and then the pellet was washed with buffer. Finally, the remaining pellet was resuspended in TMMET buffer ("P" fraction). Protein from S and P fractions were mixed with DTT and LDS, boiled at 70˚C for 10 minutes, and run on a NuPAGE 10% Bis-Tris gels in SDS running. Protein was transferred to PVDF membrane, blocked in 5% milk in PBST, incubated in beta tubulin primary (1:1000, CST 2146S) or actin C4 (1:1000, Sigma MAB1501) overnight at 4˚C. Blots were washed 3x10 minutes in PBST, incubated in secondary antibody diluted in 1% milk with 1% BSA (Goat anti-rabbit IgG HRP conjugate, Invitrogen, G21234, 1:5000; Goat anti-mouse IgG HRP conjugate, Invitrogen, 31430, 1:5000) for 1 h at RT. Blots were washed 3x 10 minutes in PBST and then incubated with Pico Chemiluminescent substrate (Invitrogen) and imaged on a Syngene G:BOX.

Statistical Analysis

Data was collected and organized in Excel, and then graphed and analyzed with GraphPad Prism Version 9.5.1 (528). Superplots were made and analyzed according to (Lord et al., 2020) where statistics were performed on the averages of 3 trials and individual trials are represented by corresponding symbol colors. For experiments, "n" is the number of cells quantified and "N" is the number of experiments.

ACKNOWLEDGEMENTS

We would like to thank the Barlowe Lab at Dartmouth College for their feedback on experimental ideas and Ann Lavanway at the Dartmouth Imaging Facility for help with microscopy. We would also like to thank the Biochemistry and Cell Biology Department at Dartmouth College for providing resources to complete this work. This work was funded by NIH MIRA R35GM128702(PA).

REFERENCES

Alushin, G. M., Lander, G. C., Kellogg, E. H., Zhang, R., Baker, D., & Nogales, E. (2014). High-Resolution Microtubule Structures Reveal the Structural Transitions in αβ-Tubulin upon GTP Hydrolysis. *Cell*, *157*(5), 1117–1129. https://doi.org/10.1016/j.cell.2014.03.053

Boyd, J. S., Gray, M. M., Thompson, M. D., Horst, C. J., & Dieckmann, C. L. (2011). The daughter four-membered microtubule rootlet determines anterior-posterior positioning of the eyespot in Chlamydomonas reinhardtii. *Cytoskeleton*, n/a-n/a. https://doi.org/10.1002/cm.20524

523 Chew, Y. M., & Cross, R. A. (2023). *Taxol acts differently on different tubulin isotypes*
524 [Preprint]. Cell Biology. https://doi.org/10.1101/2023.02.07.527540
525 Craft, J. M., Harris, J. A., Hyman, S., Kner, P., & Lechtreck, K. F. (2015). Tubulin
526 transport by IFT is upregulated during ciliary growth by a cilium-autonomous
527 mechanism. *Journal of Cell Biology*, *208*(2), 223–237.
528 https://doi.org/10.1083/jcb.201409036
529 de Forges, H., Bouissou, A., & Perez, F. (2012). Interplay between microtubule
530 dynamics and intracellular organization. *The International Journal of*
531 *Biochemistry & Cell Biology*, *44*(2), 266–274.
532 https://doi.org/10.1016/j.biocel.2011.11.009
533 Derry, W. B., Wilson, L., & Jordan, M. A. (1998). Low potency of taxol at microtubule
534 minus ends: Implications for its antimitotic and therapeutic mechanism. *Cancer*
535 *Research*, *58*(6), 1177–1184.
536 Dougherty, L. L., Dutta, S., & Avasthi, P. (2023). The ERK activator, BCI, inhibits
537 ciliogenesis and causes defects in motor behavior, ciliary gating, and cytoskeletal
538 rearrangement. *Life Science Alliance*, *6*(6), e202301899.
539 https://doi.org/10.26508/lsa.202301899
540 Dutcher, S. K., & O'Toole, E. T. (2016). The basal bodies of Chlamydomonas reinhardtii.
541 *Cilia*, *5*(1), 18. https://doi.org/10.1186/s13630-016-0039-z
542 Finst, R. J., Kim, P. J., & Quarmby, L. M. (1998). Genetics of the Deflagellation Pathway
543 in Chlamydomonas. *Genetics*, *149*(2), 927–936.
544 https://doi.org/10.1093/genetics/149.2.927

Forcioli-Conti, N., Estève, D., Bouloumié, A., Dani, C., & Peraldi, P. (2016). The size of the primary cilium and acetylated tubulin are modulated during adipocyte differentiation: Analysis of HDAC6 functions in these processes. *Biochimie*, *124*, 112–123. https://doi.org/10.1016/j.biochi.2015.09.011

Jensen, C. G., Davison, E. A., Bowser, S. S., & Rieder, C. L. (1987). Primary cilia cycle in PtK1 cells: Effects of colcemid and taxol on cilia formation and resorption. *Cell Motility and the Cytoskeleton*, *7*(3), 187–197. https://doi.org/10.1002/cm.970070302

Jordan, M. A., Toso, R. J., Thrower, D., & Wilson, L. (1993). Mechanism of mitotic block and inhibition of cell proliferation by taxol at low concentrations. *Proceedings of the National Academy of Sciences*, *90*(20), 9552–9556. https://doi.org/10.1073/pnas.90.20.9552

Kozminski, K. G., Johnson, K. A., Forscher, P., & Rosenbaum, J. L. (1993). A motility in the eukaryotic flagellum unrelated to flagellar beating (Chlamydomonas/ntrelular movement/ultrastcture). *Proc. Natl. Acad. Sci. USA*, *90*(June), 5519–5523.

Lord, S. J., Velle, K. B., Dyche Mullins, R., & Fritz-Laylin, L. K. (2020). SuperPlots: Communicating reproducibility and variability in cell biology. *Journal of Cell Biology*, *219*(6). https://doi.org/10.1083/JCB.202001064

Mitchison, T., & Kirschner, M. (1984). Dynamic instability of microtubule growth. *Nature*, *312*(5991), 237–242. https://doi.org/10.1038/312237a0

Nakamura, S., Takino, H., & Kojima, M. K. (1987). Effect of lithium on flagellar length in Chlamydomonas reinhardtii. *Cell Structure and Function*, *12*(4), 369–374. https://doi.org/10.1247/csf.12.369

O'Brien, E. T., Salmon, E. D., & Erickson, H. P. (1997). How calcium causes microtubule depolymerization. *Cell Motility and the Cytoskeleton*, *36*(2), 125–135. https://doi.org/10.1002/(SICI)1097-0169(1997)36:2<125::AID-CM3>3.0.CO;2-8

Parker, A. L., Kavallaris, M., & McCarroll, J. A. (2014). Microtubules and Their Role in Cellular Stress in Cancer. *Frontiers in Oncology*, *4*. https://doi.org/10.3389/fonc.2014.00153

Quarmby, L., & Hartzell, H. (1994). Two distinct, calcium-mediated, signal transduction pathways can trigger deflagellation in Chlamydomonas reinhardtii. *Journal of Cell Biology*, *124*(5), 807–815. https://doi.org/10.1083/jcb.124.5.807

Quarmby, L. M. (1996). Ca2+ influx activated by low pH in Chlamydomonas. *Journal of General Physiology*, *108*(4), 351–361. https://doi.org/10.1085/jgp.108.4.351

Reiter, J. F., & Leroux, M. R. (2017). Genes and molecular pathways underpinning ciliopathies. *Nature Reviews Molecular Cell Biology*, *18*(9), 533–547. https://doi.org/10.1038/nrm.2017.60

Rosenbaum, J. L., & Carlson, K. (1969). Cilia regeneration in Tetrahymena and its inhibition by colchicine. *The Journal of Cell Biology*, *40*(2), 415–425. https://doi.org/10.1083/jcb.40.2.415

Rosenbaum, J. L., Moulder, J. E., & Ringo, D. L. (1969). Flagellar elongation and shortening in Chlamydomonas: The Use of Cycloheximide and Colchicine to Study the Synthesis and Assembly of Flagellar Proteins. *Journal of Cell Biology*, *41*(2), 600–619. https://doi.org/10.1083/jcb.41.2.600

589 Sharma, N., Kosan, Z. A., Stallworth, J. E., Berbari, N. F., & Yoder, B. K. (2011). Soluble
590 levels of cytosolic tubulin regulate ciliary length control. *Molecular Biology of the*
591 *Cell*, *22*(6), 806–816. https://doi.org/10.1091/mbc.e10-03-0269
592 Stubblefield, E., & Brinkley, B. R. (1966). CILIA FORMATION IN CHINESE HAMSTER
593 FIBROBLASTS IN VITRO AS A RESPONSE TO COLCEMID TREATMENT.
594 *Journal of Cell Biology*, *30*(3), 645–652. https://doi.org/10.1083/jcb.30.3.645
595 Tripathi, P., Zhu, Z., Qin, H., Elsherbini, A., Crivelli, S. M., Roush, E., Wang, G.,
596 Spassieva, S. D., & Bieberich, E. (2021). Palmitoylation of acetylated tubulin and
597 association with ceramide-rich platforms is critical for ciliogenesis. *Journal of*
598 *Lipid Research*, *62*, 100021. https://doi.org/10.1194/jlr.RA120001190
599 Tucker, R. W., Pardee, A. B., & Fujiwara, K. (1979). Centriole ciliation is related to
600 quiescence and DNA synthesis in 3T3 cells. *Cell*, *17*(3), 527–535.
601 https://doi.org/10.1016/0092-8674(79)90261-7
602 Wang, L., Piao, T., Cao, M., Qin, T., Huang, L., Deng, H., Mao, T., & Pan, J. (2013).
603 Flagellar regeneration requires cytoplasmic microtubule depolymerization and
604 kinesin-13. *Journal of Cell Science*, *126*(6), 1531–1540.
605 https://doi.org/10.1242/jcs.124255
606 Wingfield, J. L., Mekonnen, B., Mengoni, I., Liu, P., Jordan, M., Diener, D., Pigino, G., &
607 Lechtreck, K. (2021). *In vivo* imaging shows continued association of several IFT-
608 A, IFT-B and dynein complexes while IFT trains U-turn at the tip. *Journal of Cell*
609 *Science*, *134*(18), jcs259010. https://doi.org/10.1242/jcs.259010
610 Witman, G. B., Carlson, K., Berliner, J., & Rosenbaum, L. (1972). I. Isolation and
611 Electrophoretic Analysis of Microtubules, Matrix, Membranes, and

Mastigonemes. *The Journal of Cell Biology*, *54*, 507–539.
https://doi.org/10.1083/jcb.54.3.507